Published in final edited form as:
Cell Metab. 2009 October ; 10(4): 249–259. doi:10.1016/j.cmet.2009.08.013.

MyD88 signaling in the CNS is required for development of fatty acid induced leptin resistance and diet-induced obesity

André Kleinridders[1,*], **Dominik Schenten**[2,*], **A. Christine Könner**[1,*], **Bengt F. Belgardt**[1,*], **Jan Mauer**[1], **Tomoo Okamura**[1], **F. Thomas Wunderlich**[1], **Ruslan Medzhitov**[2], and **Jens C. Brüning**[1]

[1]Department of Mouse Genetics and Metabolism, Institute for Genetics, Cologne Excellence Cluster on Cellular Stress Responses in Aging Associated Diseases (CECAD) and Center of Molecular Medicine Cologne (CMMC) University of Cologne, and 2nd Department for Internal Medicine University Hospital Cologne, Max Planck Institute for the Biology of Ageing, D-50674 Cologne, Germany

[2]Howard Hughes Medical Institute and Department of Immunobiology, Yale University School of Medicine, New Haven, Connecticut 06520, USA

Summary

Obesity-associated activation of inflammatory pathways represents a key step in the development of insulin resistance in peripheral organs, partially via activation of TLR-4 signaling by fatty acids. Here we demonstrate that palmitate acting in the central nervous system (CNS) inhibits leptin-induced anorexia and Stat-3 activation. To determine the functional significance of TLR signaling in the CNS in the development of leptin resistance and diet-induced obesity *in vivo*, we have characterized mice deficient for the TLR adaptor molecule MyD88 in the CNS ($MyD88^{\Delta CNS}$). Compared to control mice, $MyD88^{\Delta CNS}$ mice are protected from high-fat diet (HFD)-induced weight gain, from the development of HFD-induced leptin resistance and from the induction of leptin resistance by acute central application of palmitate. Moreover, CNS-restricted MyD88 deletion protects from HFD- and icv palmitate-induced impairment of peripheral glucose metabolism. Thus, we define neuronal MyD88-dependent signaling as a key regulator of diet-induced leptin and insulin resistance *in vivo*.

Introduction

The vast majority of obese patients develop obesity in the presence of increased circulating plasma leptin concentrations indicative of leptin resistance in these subjects (Frederich et al., 1995). Similarly, mice exposed to high-fat diet as a model of obesity develop hyperphagia in the presence of increased plasma leptin concentrations. Besides reduced transport of leptin across the blood/brain-barrier, impaired neuron-autonomous leptin action causes leptin resistance (El-Haschimi et al., 2000). Nevertheless, the molecular mechanisms underlying leptin resistance under conditions of obesity remain elusive.

Address correspondence to: Jens C. Brüning, M.D., Institute for Genetics, Department of Mouse Genetics and Metabolism, Zülpicher Straße 47, 50674 Köln, Germany, Phone: +49-221 470 2467, Fax: +49-221 470 5185, jens.bruening@uni-koeln.de.
*These authors contributed equally to the present study

Impairment of leptin-stimulated JAK2 activation and subsequent Stat3 and PI3k-signaling has been shown to result from increased expression and activation of inhibitors of leptin signaling such as suppressor of cytokine signaling (SOCS)3 or the protein tyrosine phosphatase PTP-1b (Bence et al., 2006; Bjorbaek et al., 1999). Accordingly, CNS-wide as well as POMC-neuron-restricted SOCS-3 ablation as well as CNS-wide ablation of PTP-1b protects from high-fat diet-induced leptin resistance (Bence et al., 2006; Kievit et al., 2006; Mori et al., 2004)

Besides the occurrence of leptin resistance, obesity is also characterized by the development of insulin resistance in the CNS (Belgardt et al., 2008; Plum et al., 2006a; Plum et al., 2005). Since insulin action in the CNS not only contributes to control of body weight (Bruning et al., 2000; Schwartz and Porte, 2005; Schwartz et al., 2000; Woods et al., 1979), but importantly also to control of peripheral glucose metabolism (Koch et al., 2008; Konner et al., 2007; Obici et al., 2002), central insulin resistance represents an important aspect in the pathophysiology of the metabolic syndrome.

The last decade has revealed important new insights into the role of innate immune response pathways in the development of obesity-associated peripheral insulin resistance. Both macrophage recruitment to white adipose tissue and adipocyte autonomous release of proinflammatory cytokines, resulting in activation of JNK- and IKK-signaling pathways, which interfere with insulin signaling in classical insulin target tissues such as liver and skeletal muscle (Arkan et al., 2005; Cai et al., 2005; Hirosumi et al., 2002; Hotamisligil et al., 1993; Rohl et al., 2004; Shoelson et al., 2003; Uysal et al., 1997; Weisberg et al., 2003; Wunderlich et al., 2008; Xu et al., 2003). Both pharmacological and genetic intervention with these signaling pathways has been shown to improve glucose metabolism (Arkan et al., 2005; Cai et al., 2005; Hirosumi et al., 2002; Hotamisligil et al., 1993; Shoelson et al., 2003; Uysal et al., 1997; Wunderlich et al., 2008). Moreover, metabolic disturbances associated with obesity such as hyperlipidemia and hyperglycemia also activate JNK, IKK and atypical PKCs (Chibalin et al., 2008; Hirosumi et al., 2002; Shoelson et al., 2003).

Saturated fatty acids can also serve as ligands for TLR4 in addition to the well-characterized bacterial lipopolysaccharides initially identified as TLR ligands (Lee et al., 2001; Shi et al., 2006). Mice with either targeted disruption or naturally occurring mutations of TLR4 are protected from obesity-associated insulin resistance (Poggi et al., 2007; Shi et al., 2006; Tsukumo et al., 2007). Interestingly, genetic models interfering with inflammatory signaling such as conventional JNK1- and TLR4-deficient mice are not only protected from the occurrence of obesity-associated insulin resistance, but also from weight gain, although these effects have so far not been studied in greater detail (Hirosumi et al., 2002). More recently, activation of inflammatory signaling has also been detected in the hypothalamus of obese rats (De Souza et al., 2005). It was subsequently demonstrated that inhibiting IKK2 action in the CNS (Zhang et al., 2008) or ameliorating ER-stress activation in the CNS (Ozcan et al., 2009) prevents neuronal leptin resistance, and two very recent studies indicated that short-term pharmacological inhibition of neuronal TLR-signaling inhibits fatty acid-induced insulin (Posey et al., 2009) and leptin resistance (Milanski et al., 2009).

MyD88 is an essential signaling adaptor for most TLRs and for members of the IL-1 receptor family (Kawai et al., 1999). TLR4 signaling specifically depends on the signaling adaptor TRIF in addition to MyD88. However, while TRIF is required for the induction of TLR3- and TLR4-induced type I interferons, MyD88 is essential for the induction of proinflammatory cytokines (Kawai and Akira, 2006; Yamamoto et al., 2003). Therefore, we have generated and analyzed mice that carry a CNS-specific ablation of MyD88, in order to address the role of fatty acids acting in the CNS in general, and TLR-mediated MyD88-

dependent signaling in the development of obesity and obesity-associated insulin resistance specifically.

Results

Palmitate can induce leptin resistance in the CNS

To directly address whether saturated fatty acids can impair central leptin action *in vivo*, we aimed to investigate the acute pharmacological effect of intracerebroventricularly (icv) applied palmitate on the anorectic effect of leptin. First, we monitored whether different doses of palmitate affected food intake in a re-feeding paradigm. This analysis revealed that in a range from 10–66 pmol, icv palmitate had no acute effect on food intake compared to injection of the BSA-carrier solution (Fig. 1A). Next, we confirmed, that injection of carrier solution 30 minutes prior to leptin application compared to carrier solution application followed by saline injection resulted in a significant reduction of food intake by 60% (Fig. 1B), comparable to the described acute anorectic effect of icv leptin treatment in control mice (Mistry et al., 1997). However, although injection of 66 pmol palmitate prior to saline injection resulted in a comparable food intake as observed in animals receiving saline injection after BSA injection (Fig. 1B), leptin injection following pretreatment with palmitate failed to significantly reduce food intake in these mice (Fig. 1B).

Next, we addressed, whether icv palmitate treatment directly affects leptin evoked hypothalamic signaling. Therefore, we investigated leptin's ability to activate Stat3 phosphorylation after icv pretreatment of mice with either BSA-containing carrier solution or 66 pmol palmitate. While leptin stimulation subsequent to an icv injection of BSA-carrier profoundly activated Stat3 phosphorylation in the hypothalamus of mice (Fig. 1C), this response was blunted by 60% after icv palmitate treatment (Fig. 1C). Taken together, these experiments indicate that palmitate treatment acutely inhibits both leptin-evoked Stat3-phosporylation and leptin induced anorexia *in vivo*.

Generation of MyD88$^{\Delta CNS}$ mice

In peripheral tissues fatty acids have been demonstrated to cause insulin resistance and to activate inflammatory pathways in a TLR4-dependent manner (Shi et al., 2006). Thus, we next aimed to directly address the contribution of TLR-dependent signaling in the CNS to the development of fatty acid-induced leptin resistance and high-fat diet-induced obesity *in vivo*. To this end, we generated mice that carry a CNS-specific ablation of the principal TLR-adaptor molecule MyD88 (MGI: 108005), which is essential for both TLR-dependent JNK and IKK activation (Suppl. Fig. 1A) (Adachi et al., 1998; Janssens and Beyaert, 2002).

Western blot analysis revealed strongly reduced amounts of immunoreative MyD88 protein in extracts isolated from brain of brain-specific MyD88 knockout (MyD88$^{\Delta CNS}$) mice compared to control animals (Suppl. Fig. 1B), while MyD88-expression remained unaltered in peripheral tissues of MyD88$^{\Delta CNS}$ mice compared to controls (Suppl. Fig. 1C), thus demonstrating the successful generation of brain-specific MyD88 knockout mice.

Normal energy homeostasis in MyD88$^{\Delta CNS}$ mice

To investigate whether deletion of MyD88 in the CNS affected body weight regulation or glucose metabolism in mice exposed to normal chow diet, we next monitored parameters of energy homeostasis and glucose metabolism in MyD88$^{\Delta CNS}$ mice compared to controls. These analyses revealed unaltered body weight, body length, epigonadal fat pad mass, as well as unaltered histomorphological appearance of white adipose tissue in MyD88$^{\Delta CNS}$ mice compared to controls both in male and female mice at the age of 16 weeks (Fig. 2A–H). Similarly, analysis of blood glucose and plasma insulin concentrations as well as glucose

and insulin tolerance tests revealed unaltered glucose metabolism in MyD88$^{\Delta CNS}$ compared to control mice (Fig. 3A–F). Taken together these experiments indicate that MyD88-dependent signaling in the CNS is dispensable for maintenance of body weight and glucose homeostasis in lean mice.

MyD88$^{\Delta CNS}$ mice are protected from HFD-induced weight gain

To directly investigate the role of MyD88-dependent signaling in the CNS in the development of diet-induced obesity, we next monitored body weight in control and MyD88$^{\Delta CNS}$ mice, which were exposed to high fat containing diet (HFD) from 3 weeks of age on. Strikingly, while HFD-induced weight gain was significantly attenuated in male MyD88$^{\Delta CNS}$ mice compared to control mice (Fig. 2A, Suppl. Fig. 2A); it was completely abolished in female MyD88$^{\Delta CNS}$ mice (Fig. 2B, Suppl. Fig. 2B). Similarly, while high fat feeding increased body length in control mice, presumably via impairment of MC4R action (Yaswen et al., 1999) (Huszar et al., 1997), this effect was abolished in MyD88$^{\Delta CNS}$ mice (Fig. 2C, D). While epigonadal fat pad mass was only slightly reduced in male MyD88$^{\Delta CNS}$ mice (Fig. 2E) and overall fat content remained unaltered in male MyD88$^{\Delta CNS}$ mice compared to controls (Suppl. Fig. 2C), female MyD88$^{\Delta CNS}$ mice exhibited a significant 60% reduction in the amount of parametrial fat mass (Fig. 2F) and a significant 24% reduction in body fat content (Suppl. Fig. 2D) compared to controls upon high fat feeding. Unlike in control mice, in which exposure to high-fat diet resulted in significant enlargement of adipocytes in WAT in both control male and female mice, adipocyte hyperplasia upon high fat feeding was completely prevented in MyD88$^{\Delta CNS}$ mice of both genders (Fig. 2G, H). Taken together, brain-specific disruption of MyD88 protects from HFD-induced weight gain, from increase in body length and white adipose tissue (WAT) remodeling in both genders, while it prevents overall fat accumulation only in female mice.

Improved energy homeostasis in MyD88$^{\Delta CNS}$ mice

To investigate the mechanism(s) underlying protection from HFD-induced weight gain in MyD88$^{\Delta CNS}$ mice, we next monitored caloric intake of these animals both at the age of 4 weeks, when body weights between controls and MyD88$^{\Delta CNS}$ mice were still indistinguishable and at the age of 12 weeks, when MyD88$^{\Delta CNS}$ mice showed already reduced body weight compared to controls. While both male and female MyD88$^{\Delta CNS}$ mice exhibited a trend towards reduced food intake at 4 weeks of age, only male MyD88$^{\Delta CNS}$ mice consumed significantly less food compared to controls at the age of 12 weeks (Fig. 4A, B). On the other hand, energy expenditure as assessed by oxygen production corrected per lean body mass during indirect calorimetry was not significantly altered in female MyD88$^{\Delta CNS}$ mice compared to controls both at 4 and 12 weeks of age and male MyD88$^{\Delta CNS}$ mice only exhibited increased energy expenditure during nighttime at 12 weeks of age (Fig. 4C, D). Moreover, there were no consistent, significant alterations in spontaneous locomotor activity in MyD88$^{\Delta CNS}$ mice (Fig. 4E, F). Thus, the mechanism underlying protection from HFD-induced obesity in MyD88$^{\Delta CNS}$ mice likely is caused primarily by reduced food intake of MyD88$^{\Delta CNS}$ mice.

MyD88$^{\Delta CNS}$ mice exhibit increased leptin sensitivity

Given the occurrence of leptin resistance upon acute palmitate injection in control mice and the protection of MyD88$^{\Delta CNS}$ mice from HFD-induced weight gain, we next asked whether leptin action is altered in MyD88$^{\Delta CNS}$ mice. Therefore, we subjected control and MyD88$^{\Delta CNS}$ mice, which had been exposed to HFD to twice-daily injections of mouse recombinant leptin following a series of twice daily saline injections. Leptin failed to significantly reduce food intake in female control mice, but it significantly reduced food intake in female MyD88$^{\Delta CNS}$ mice exposed to HFD (Fig. 5A). Similarly, while leptin reduced food intake in male control mice by 13.4 % it significantly reduced food intake in

male MyD88$^{\Delta CNS}$ mice by 34.2 % (Suppl. Fig. 3). Similarly, acute intravenous injection of leptin failed to significantly activate Stat3-phosphorylation in the arcuate nucleus of control mice exposed to HFD, whereas leptin's ability to activate Stat3 phosphorylation was restored in MyD88$^{\Delta CNS}$ mice (Fig. 5B, C). Since restoration of leptin sensitivity in mice, which are protected from HFD-induced weight gain may be confounded by the reduced body weight, we next performed similar experiments in mice, which had been exposed to HFD only for two weeks and thus at the time of assessing leptin sensitivity still exhibited comparable body weight (Fig. 5D). While leptin treatment still inhibited food intake in control mice, which had been exposed to HFD for two weeks, by 30%, the anorexigenic action of leptin in MyD88$^{\Delta CNS}$ mice exposed to HFD for the same period was significantly more pronounced and reduced food intake by 55% (Fig. 5E). Thus, disruption of MyD88-dependent signaling in the CNS improved leptin sensitivity in mice exposed to high caloric diet, even before differences in body weight were present. On the other hand, while MyD88$^{\Delta CNS}$ mice exhibited an improved response to leptin, steady state mRNA expression of POMC, NPY, and AgRP remained unaltered in MyD88$^{\Delta CNS}$ mice compared to controls (Suppl. Fig. 4).

Given the reversal of HFD-induced leptin resistance in MyD88$^{\Delta CNS}$ mice with respect to both Stat3-phosphorylation and anorexigenic action, we next aimed to investigate whether CNS-restricted MyD88 deletion also affects the ability of palmitate to inhibit leptin-stimulated Stat3-phosphorylation upon injection. To this end, we compared the effect of combined icv treatment with palmitate and leptin in lean control and MyD88$^{\Delta CNS}$ mice. Interestingly, disruption of MyD88 largely enhanced hypothalamic leptin-stimulated Stat3 phosphorylation in the presence of palmitate in MyD88$^{\Delta CNS}$ compared to control mice (Fig. 5F), indicating that palmitate-evoked leptin resistance is mediated by MyD88-dependent signaling. Taken together, these data clearly show that MyD88 in the CNS is a critical mediator of leptin resistance evoked both by high fat feeding and by acute administration of saturated fatty acids *in vivo*.

To further investigate, whether reduced weight gain of MyD88$^{\Delta CNS}$ mice in response to high fat feeding is only accompanied by improved leptin action, or whether these animals may exhibit different responses to other anorexigenic signals, we next compared the anorexigenic and body weight reducing effect of the melanocortin (MC)-4 receptor agonist melanotan (MT II). This analysis revealed improved anorexigenic and weight reducing effect of MTII in MyD88$^{\Delta CNS}$ mice compared to controls (Fig. 5G). Thus, MyD88 disruption not only improved leptin but also melanocortin signaling in mice exposed to high-fat diet.

Ameliorated IKK activation in MyD88$^{\Delta CNS}$ mice

To investigate whether obesity-induced IKK- and possibly JNK-activation in the hypothalamus occurs as a consequence of fatty acid-activated, TLR- and MyD88-dependent signaling, we compared the expression and activation of IKKs and JNK in the hypothalami of control and MyD88$^{\Delta CNS}$ mice, which had been exposed for 12 weeks to HFD. Immunoblot analysis with antibodies, which recognize IKKs, when phosphorylated at serine residues 176/180 as a marker of activation (DiDonato et al., 1997), revealed a significant amount of activated IKKs in extracts of arcuate nuclei of control mice, while IKK-phosphorylation was slightly reduced in extracts isolated from MyD88$^{\Delta CNS}$ mice, even though total immunoreactive IKKs were clearly in the extracts of MyD88$^{\Delta CNS}$ mice (Fig. 6A). Next we investigated the regulation of IκBα-expression and -phosphorylation. IKK-dependent phosphorylation targets IκBα for proteasomal degradation, thus allowing for nuclear translocation of NFκB. Comparison of IκBα-expression in hypothalamic extracts from HFD-fed control and MyD88$^{\Delta CNS}$ mice revealed a significant increase of IκBα-

expression but significantly reduced phosphorylation in hypothalamic extracts from MyD88$^{\Delta CNS}$ mice compared to controls (Fig. 6B). Taken together, these data clearly demonstrate that MyD88 deletion reduces IKK-activation in the hypothalamus of obese mice.

In contrast, analysis of JNK-phosphorylation in hypothalami of MyD88$^{\Delta CNS}$ mice revealed both a significant decrease in immunoreactive phosphorylated as well as total JNK-protein compared to controls (Fig. 6C). Thus, JNK-activation remained unaltered in MyD88$^{\Delta CNS}$ mice. Similar to JNK-activation, expression of proinflammatory cytokines such as TNF and IL-6 as well as markers of ER-stress, such as GRP78, spliced XBP and CHOP remained unaltered in HFD-fed MyD88$^{\Delta CNS}$ mice compared to controls (Suppl. Fig. 5A, B).

Thus, improved leptin sensitivity in the presence of unaltered JNK-activity, indicated that JNK-activation is not responsible for induction of diet-induced leptin resistance. Since hypothalamic JNK-activation occurs upon HFD-induced obesity (De Souza et al., 2005; Won et al., 2009) (B. F. Belgardt and J. C. Brüning, unpublished) and to directly test the role of JNK-dependent signaling in the development of diet-induced leptin-resistance, we compared the food intake- and body weight-reducing effect of leptin in control mice and those with targeted disruption of JNK1 specifically in the CNS (B. F. Belgardt and J. C. Brüning, unpublished). This analysis indicated that leptin failed to significantly reduce both food intake and body weight in either control or brain-specific JNK1 knockout mice exposed to HFD (Fig. 6D), consistent with unaltered food intake and body composition of these mice upon HFD exposure (B. F. Belgardt and J. C. Brüning, unpublished). Taken together, MyD88 ablation in the CNS abrogates high-fat diet-induced IKK-, but not JNK-activation in the hypothalamus of mice, assigning MyD88-dependent signaling a crucial role in diet-induced inflammatory signaling not only in peripheral tissues, but also in the CNS.

Improved insulin action in MyD88$^{\Delta CNS}$ mice

To investigate the effect of CNS-specific disruption of MyD88 and subsequently that of IKK-activation in the hypothalamus on peripheral glucose metabolism upon exposure to HFD, we next compared blood glucose and plasma insulin concentrations in control and MyD88$^{\Delta CNS}$ mice. While control mice exposed to HFD developed significantly impaired glucose in the presence of pronounced hyperinsulinemia compared to mice exposed to NCD (Fig. 3A–F), HFD-induced impairment of glucose and insulin tolerance as well as insulin concentrations was largely blunted in male and female MyD88$^{\Delta CNS}$ mice (Fig. 3A–F). Taken together, ablation of the TLR adapter MyD88 in the CNS ameliorated whole body insulin sensitivity during the course of diet-induced obesity.

To further investigate the contribution of chronic MyD88-dependent, palmitate-evoked signaling in the CNS to the phenotype of HFD-fed animals, we next compared the effect of chronic palmitate icv infusion over a period of 2 weeks in control and MyD88$^{\Delta CNS}$ mice. While in control animals palmitate infusion did not significantly alter fat mass and food intake over the 2 week period (Fig. 7A, B), central palmitate infusion compared to BSA infusion significantly impaired insulin tolerance in control mice (Fig. 7C). Strikingly, while brain-specific disruption of MyD88 again did not affect fat mass and food intake in palmitate-infused animals (Fig. 7D, E), palmitate-induced insulin resistance was blunted in MyD88$^{\Delta CNS}$ mice compared to controls (Fig. 7F).

Discussion

Resistance to leptin and insulin action in the CNS represents a hallmark during the development of high caloric diet-induced weight gain and peripheral insulin resistance (Schwartz and Porte, 2005). Here we demonstrate that palmitate, an abundant fatty acid in

the circulation, which is also increased in the hypothalamus upon high fat feeding (Posey et al., 2008), acutely causes leptin resistance in the CNS. These findings extend those recently published by Milanski et al., demonstrating that central application of stearic and arachidic acid activate proinflammatory gene expression in the hypothalamus in a TLR-dependent manner (Milanski et al., 2009).

Saturated fatty acids represent important candidates for causing diet-induced leptin and insulin resistance. Saturated, but not unsaturated fatty acids act as ligands for TLR4 (Lee et al., 2001), thus activating JNK- and IKK-signaling cascades, both of which inhibit insulin action (Hirosumi et al., 2002) (Arkan et al., 2005).

Consistent with a role for palmitate in obesity-associated insulin resistance, there is evidence that mice with impaired TLR4 expression are protected from obesity-associated insulin resistance (Poggi et al., 2007; Shi et al., 2006; Tsukumo et al., 2007), while body weight under HFD conditions is either increased (Shi et al., 2006), decreased (Tsukumo et al., 2007) or unchanged (Kim et al., 2007; Poggi et al., 2007) in these animals compared to controls. The reasons for these different findings are unclear, but may be accounted for by different genetic backgrounds, diet composition or different environmental factors. Interestingly, TLR4 disruption selectively protected from high-fat diet-induced insulin resistance caused by saturated, but not unsaturated fatty acids (Davis et al., 2008), consistent with a pivotal role for palmitate in high fat-diet-induced, obesity-associated insulin resistance. Disruption of TLR2 also protects from obesity-associated insulin resistance and palmitate-induced insulin resistance in cultured skeletal muscle cells (Senn, 2006) (Caricilli et al., 2008). These experiments point towards redundancy among different TLRs in mediating the insulin resistance inducing effect of fatty acids. Consistent with redundant action of TLR2 and TLR4 in fatty acid-induced gene expression, Milanski et al. demonstrate that both TLR2- and TLR4-blocking antibodies attenuate fatty acid induction of hypothalamic proinflammatory gene expression (Milanski et al., 2009).

Our experiments directly demonstrate that the pharmacological effect of palmitate in causing leptin resistance depends on MyD88-activated signaling. Since MyD88 serves as an adaptor molecule to mediate both TLR and IL-1-receptor activated NFκB- and JNK-signaling, our experiments cannot formally exclude the possibility that palmitate-induced leptin resistance is mediated by the IL-1 receptor. While leptin-induced anorexia has been demonstrated to be abolished in IL-1 receptor knockout mice (Luheshi et al., 1999), physiological effects of leptin on energy balance seem to be independent of IL-1 signaling (Wisse et al., 2007). Nevertheless, impairment of IL-1 signaling in MyD88$^{\Delta CNS}$ mice probably does not account for leptin sensitization in these animals. Taken together with the experiments on TLR-blocking antibodies (Milanski et al., 2009), we conclude that palmitate induces leptin resistance via TLR-activated MyD88-dependent signals.

Our study also offers important evidence for the nature of the downstream mediator of palmitate-induced, MyD88-dependent leptin resistance upon high fat feeding. Only activation of IKK, deletion of which in the CNS has recently been demonstrated to rescue obesity-associated leptin resistance (Zhang et al., 2008), is significantly reduced in hypothalami of MyD88$^{\Delta CNS}$ mice exposed to high-fat diet. Although JNK signaling also represents a candidate pathway for palmitate-mediated leptin resistance, i.e. via stimulation of inhibitory serine phosphorylation of Stat3 (Lim and Cao, 1999), the presence of unaltered JNK-activation in hypothalami of MyD88$^{\Delta CNS}$ mice, which are protected from obesity, indicates that JNK signaling is not responsible for mediating leptin resistance upon HFD-feeding in these mice. Importantly, this notion is further directly supported by our experiments, revealing that CNS-specific disruption of JNK1 fails to improve diet-induced

leptin resistance. Moreover, our experiments indicate that stimuli other than palmitate in MyD88-deficient mice are responsible for high-fat diet-induced chronic JNK-activation.

Consistent with the role of palmitate- and diet-induced, MyD88-dependent IKK-activation in causing leptin resistance, Posey et al recently demonstrated that palmitate can acutely cause insulin resistance in the CNS and that this effect can be reversed by pharmacological inhibition of IKK-dependent signaling (Posey et al., 2008). Although the authors of this study do not provide evidence for the signaling pathway involved, our results clearly indicate that palmitate-induced IKK-activation and IκBα degradation critically depend on MyD88. On the other hand, the absence of alterations in proinflammatory gene expression in our model, argue for a role of IKK-dependent, but potentially NFkB-independent signaling in the induction of insulin and leptin resistance. Alternatively, unaltered JNK-activation may account for unaltered proinflammatory gene expression even in the presence of reduced IKK-activation. Thus, in addition to the reversal of leptin resistance in the CNS of MyD88$^{\Delta CNS}$ mice, these animals are predicted to be protected also from palmitate induced neuronal insulin resistance. Since we and others have previously demonstrated that insulin action in the CNS (Bruning et al., 2000; Koch et al., 2008; Obici et al., 2002), particularly in AgRP-expressing neurons (Konner et al., 2007), is critical for control of peripheral glucose metabolism - mainly via suppression of hepatic glucose production - the disproportional improvement of glucose metabolism in male MyD88$^{\Delta CNS}$ mice, despite only minor reduction of fat content and body weight, indeed indicate improved insulin action in the CNS of these mice. While at this point, we cannot define the underlying mechanism for the gender-specific effect of CNS-restricted MyD88 disruption on obesity development, our data are consistent with multiple knockout experiments targeting signaling pathways involved in the regulation of energy homeostasis that yielded as-yet unexplained gender-specific phenotypes (Alfadda et al., 2004; Bruning et al., 2000; Lewitt and Brismar, 2002; Plum et al., 2006b).

Nevertheless, differential improvement of leptin and insulin sensitivity is further supported by our results obtained upon chronic icv palmitate infusion. Also in this experimental paradigm, central MyD88 deficiency preferentially restores peripheral insulin sensitivity, even when body weight regulation is not affected. The differential sensitivity of body weight regulation and control of peripheral glucose metabolism may stem from the differential responsiveness of neuronal leptin and insulin signaling towards inhibition by fatty acid-induced MyD88-dependent signaling. Thus, in the chronic infusion paradigm higher palmitate doses might be required to induce leptin resistance and weight gain in longterm as seen under high-fat diet conditions. Nevertheless, our study clearly reveals a critical role for MyD88-dependent signaling in the CNS in development of fatty acid- and high-fat diet-induced leptin and insulin resistance *in vivo*.

Moreover, the finding that neuronal MyD88 disruption also improves melanocortin sensitivity clearly deserves further studies. These findings implicate that MyD88-dependent signaling impairs leptin and insulin action in the arcuate nucleus as well as downstream neurons in the circuitry such as MC4R-positive PVN-neurons.

Intranasal application of small peptides results in selective increase of cerebrospinal concentrations without reaching significant concentrations in circulation (Born et al., 2002). Thus, this route may serve as a new approach to deliver small inhibitors of TLR/MyD88 interaction, potentially setting the ground for novel therapeutic interventions with the obesity epidemic, without impairing systemic pathogen defense mechanisms.

Experimental Procedures

Generation of MyD88$^{\Delta CNS}$ mice

The generation of the conditional allele of *MyD88* (MGI: 108005) will be described in detail in a separate publication. Briefly, the essential TIR domain-encoding exons 3–5 were flanked with *loxP* sites in C57/BL6-derived embryonic stem (ES) cells in order to render *MyD88* suceptible to Cre-mediated recombination. The resulting *MyD88^{lox}* mice were then crossed to mice expressing Cre under the CNS-specific rat nestin promoter (Bruning et al., 2000) to yield *MyD88$^{lox/lox}$; NesCre*+/− mice (termed MyD88$^{\Delta CNS}$ mice). *MyD88$^{lox/lox}$* mice were used as control. Breeding colonies were maintained by mating *MyD88$^{lox/lox}$* with *NesCre-MyD88$^{lox/lox}$* mice. *NesCre* mice had been backcrossed for at least 5 generations on a C57BL/6 background before intercrossing them with *MyD88$^{lox/lox}$* mice. Thus, C57/BL6 alleles accounted for more than 98% of genes in the experimental mice. Mice were genotyped by PCR using genomic DNA isolated from tail tips. *NesCre* primers: *NesCre 5'*: 5'-CGC TTC CGC TGG GTC ACT GTC G-3'; *NesCre 3''*: 5'- TCG TTG CAT CGA CCG GTA ATG CAG GC-3'; *MyD88* primers: Seq19: 5'- GGG AAT AAT GGC AGT CCT CTC CCA G -3', Seq20: 5'- GGA TCA TCT CCT GCA CAA ACT CG -3'. Germline deletion of *NesCre* was excluded with a deletion PCR using two primers, one binding upstream the first loxP site and the others flanking the second loxP site: Seq19: 5'- GGG AAT AAT GGC AGT CCT CTC CCA G -3', Seq16: 5'- C AGT CTC ATC TTC CCC TCT GCC -3'.

Body composition

Body fat content was measured in vivo by nuclear magnetic resonance using a minispec mq 7.5 (Bruker Optics).

Western blot analysis

Indicated tissues were dissected and homogenized in homogenization buffer with a polytron homogenizer (IKA Werke), and western blot analyses were performed as previously described (Schubert et al., 2004) with antibodies raised against MyD88 (#2068, Abcam) and α-Tubulin (#T6074, Sigma) as loading control. Arcuate nuclei were dissected and homogenized with a mortar, and western blot analyses were performed with antibodies raised against pSTAT3 (#9451, Cell Signaling), STAT3 (#4904, Cell Signaling), pIKKα/β (#2697, Cell Signaling), IKKβ (#2370, Cell Signaling), pIκBα (#9241, Cell Signaling), IκBα (#9242, Cell Signaling), JNK (#9252, Cell Signaling), pJNK (#9251, Cell Signaling), Grp78 (#sc 13968, Santa Cruz), GADD153 (CHOP) (#sc 7351, Santa Cruz), Xbp1 (# sc 7160, Santa Cruz), and β–Actin (#A5441, Sigma).

Intracerebroventricular experiments

For icv cannula implantation, 10-week-old male C57BL/6 (Charles River Laboratories), control (*MyD88$^{lox/lox}$*), and MyD88$^{\Delta CNS}$ mice were anesthetized by intraperitoneal injection of Avertin (650 mg/kg) (2,2,2-tribromoethanol; Sigma) and placed in a stereotactic device. A sterile osmotic pump connector cannula (Bilaney Consultants) was implanted into the left lateral brain ventricle (−0.2 mm anterior and 1.0 mm lateral relative to Bregma and 2.3 mm below the surface of the skull). The support plate of the catheter was attached to the skull with Super Glue (Super Glue Corp.). The catheter was prefilled with 0.9% saline and connected to a sealed microrenathane catheter (MRE-025; Braintree Scientific Inc.). After 5 days of recovery, mice were fasted overnight and the sealed microrenathane catheter was removed. Palmitate (10, 20, 50 or 66 pmol), vehicle (BSA), Leptin (500ng) or vehicle (0.9% saline) was injected in a volume of 2μl according to the respective experimental set-up (see Figure 1). The catheter was subsequently sealed to avoid backflow. Injections were

performed in isoflurane anesthesia. Palmitate solutions were prepared as previously described (Listenberger et al., 2001).

Statistical methods

Data sets were analyzed for statistical significance using a two-tailed unpaired student's T-Test. *P* values less than 0.05 were considered significant.

Supplementary Material

Refer to Web version on PubMed Central for supplementary material.

Acknowledgments

We thank Gisela Schmall and Tanja Rayle for excellent secretarial assistance, Brigitte Hampel and Jens Alber for excellent technical assistance, and Dr. Hella S. Brönneke for help with the PhenoMaster. This work was supported by the ZMMK (J.C.B.), the European Community's 7th Framework Programme (grant FP7/2007-2013, n° 201608 to J.C.B.) the DFG (grant 1492-7 to J.C.B.), the BMBF obesity competence network "Neurotarget" (to J.C.B.), the NIH (grant AI 055502 to R. M.), and the HHMI (R.M., D.S. was supported by training grant of the NIH and an Irvington fellowship of the Cancer Research Institute).

References

Adachi O, Kawai T, Takeda K, Matsumoto M, Tsutsui H, Sakagami M, Nakanishi K, Akira S. Targeted disruption of the MyD88 gene results in loss of IL-1- and IL-18-mediated function. Immunity. 1998; 9:143–150. [PubMed: 9697844]

Alfadda A, DosSantos RA, Stepanyan Z, Marrif H, Silva JE. Mice with deletion of the mitochondrial glycerol-3-phosphate dehydrogenase gene exhibit a thrifty phenotype: effect of gender. Am J Physiol Regul Integr Comp Physiol. 2004; 287:R147–R156. [PubMed: 15031134]

Arkan MC, Hevener AL, Greten FR, Maeda S, Li ZW, Long JM, Wynshaw-Boris A, Poli G, Olefsky J, Karin M. IKK-beta links inflammation to obesity-induced insulin resistance. Nat Med. 2005; 11:191–198. [PubMed: 15685170]

Belgardt BF, Husch A, Rother E, Ernst MB, Wunderlich FT, Hampel B, Klockener T, Alessi D, Kloppenburg P, Bruning JC. PDK1 deficiency in POMC-expressing cells reveals FOXO1-dependent and -independent pathways in control of energy homeostasis and stress response. Cell Metab. 2008; 7:291–301. [PubMed: 18396135]

Bence KK, Delibegovic M, Xue B, Gorgun CZ, Hotamisligil GS, Neel BG, Kahn BB. Neuronal PTP1B regulates body weight, adiposity and leptin action. Nat Med. 2006; 12:917–924. [PubMed: 16845389]

Bjorbaek C, El-Haschimi K, Frantz JD, Flier JS. The role of SOCS-3 in leptin signaling and leptin resistance. J Biol Chem. 1999; 274:30059–30065. [PubMed: 10514492]

Born J, Lange T, Kern W, McGregor GP, Bickel U, Fehm HL. Sniffing neuropeptides: a transnasal approach to the human brain. Nat Neurosci. 2002; 5:514–516. [PubMed: 11992114]

Bruning JC, Gautam D, Burks DJ, Gillette J, Schubert M, Orban PC, Klein R, Krone W, Muller-Wieland D, Kahn CR. Role of brain insulin receptor in control of body weight and reproduction. Science. 2000; 289:2122–2125. [PubMed: 11000114]

Cai D, Yuan M, Frantz DF, Melendez PA, Hansen L, Lee J, Shoelson SE. Local and systemic insulin resistance resulting from hepatic activation of IKK-beta and NF-kappaB. Nat Med. 2005; 11:183–190. [PubMed: 15685173]

Caricilli AM, Nascimento PH, Pauli JR, Tsukumo DM, Velloso LA, Carvalheira JB, Saad MJ. Inhibition of toll-like receptor 2 expression improves insulin sensitivity and signaling in muscle and white adipose tissue of mice fed a high-fat diet. J Endocrinol. 2008; 199:399–406. [PubMed: 18787058]

Chibalin AV, Leng Y, Vieira E, Krook A, Bjornholm M, Long YC, Kotova O, Zhong Z, Sakane F, Steiler T, et al. Downregulation of diacylglycerol kinase delta contributes to hyperglycemia-induced insulin resistance. Cell. 2008; 132:375–386. [PubMed: 18267070]

Davis JE, Gabler NK, Walker-Daniels J, Spurlock ME. Tlr-4 deficiency selectively protects against obesity induced by diets high in saturated fat. Obesity (Silver Spring). 2008; 16:1248–1255. [PubMed: 18421279]

De Souza CT, Araujo EP, Bordin S, Ashimine R, Zollner RL, Boschero AC, Saad MJ, Velloso LA. Consumption of a fat-rich diet activates a proinflammatory response and induces insulin resistance in the hypothalamus. Endocrinology. 2005; 146:4192–4199. [PubMed: 16002529]

DiDonato JA, Hayakawa M, Rothwarf DM, Zandi E, Karin M. A cytokine-responsive IkappaB kinase that activates the transcription factor NF-kappaB. Nature. 1997; 388:548–554. [PubMed: 9252186]

El-Haschimi K, Pierroz DD, Hileman SM, Bjorbaek C, Flier JS. Two defects contribute to hypothalamic leptin resistance in mice with diet-induced obesity. J Clin Invest. 2000; 105:1827–1832. [PubMed: 10862798]

Frederich RC, Hamann A, Anderson S, Lollmann B, Lowell BB, Flier JS. Leptin levels reflect body lipid content in mice: evidence for diet-induced resistance to leptin action. Nat Med. 1995; 1:1311–1314. [PubMed: 7489415]

Hirosumi J, Tuncman G, Chang L, Gorgun CZ, Uysal KT, Maeda K, Karin M, Hotamisligil GS. A central role for JNK in obesity and insulin resistance. Nature. 2002; 420:333–336. [PubMed: 12447443]

Hotamisligil GS, Shargill NS, Spiegelman BM. Adipose expression of tumor necrosis factor-alpha: direct role in obesity-linked insulin resistance. Science. 1993; 259:87–91. [PubMed: 7678183]

Huszar D, Lynch CA, Fairchild-Huntress V, Dunmore JH, Fang Q, Berkemeier LR, Gu W, Kesterson RA, Boston BA, Cone RD, et al. Targeted disruption of the melanocortin-4 receptor results in obesity in mice. Cell. 1997; 88:131–141. [PubMed: 9019399]

Janssens S, Beyaert R. A universal role for MyD88 in TLR/IL-1R-mediated signaling. Trends Biochem Sci. 2002; 27:474–482. [PubMed: 12217523]

Kawai T, Adachi O, Ogawa T, Takeda K, Akira S. Unresponsiveness of MyD88-deficient mice to endotoxin. Immunity. 1999; 11:115–122. [PubMed: 10435584]

Kawai T, Akira S. TLR signaling. Cell Death Differ. 2006; 13:816–825. [PubMed: 16410796]

Kievit P, Howard JK, Badman MK, Balthasar N, Coppari R, Mori H, Lee CE, Elmquist JK, Yoshimura A, Flier JS. Enhanced leptin sensitivity and improved glucose homeostasis in mice lacking suppressor of cytokine signaling-3 in POMC-expressing cells. Cell Metab. 2006; 4:123–132. [PubMed: 16890540]

Kim F, Pham M, Luttrell I, Bannerman DD, Tupper J, Thaler J, Hawn TR, Raines EW, Schwartz MW. Toll-like receptor-4 mediates vascular inflammation and insulin resistance in diet-induced obesity. Circ Res. 2007; 100:1589–1596. [PubMed: 17478729]

Koch L, Wunderlich FT, Seibler J, Konner AC, Hampel B, Irlenbusch S, Brabant G, Kahn CR, Schwenk F, Bruning JC. Central insulin action regulates peripheral glucose and fat metabolism in mice. J Clin Invest. 2008; 118:2132–2147. [PubMed: 18451994]

Konner AC, Janoschek R, Plum L, Jordan SD, Rother E, Ma X, Xu C, Enriori P, Hampel B, Barsh GS, et al. Insulin action in AgRP-expressing neurons is required for suppression of hepatic glucose production. Cell Metab. 2007; 5:438–449. [PubMed: 17550779]

Lee JY, Sohn KH, Rhee SH, Hwang D. Saturated fatty acids, but not unsaturated fatty acids, induce the expression of cyclooxygenase-2 mediated through Toll-like receptor 4. J Biol Chem. 2001; 276:16683–16689. [PubMed: 11278967]

Lewitt MS, Brismar K. Gender difference in the leptin response to feeding in peroxisome-proliferator-activated receptor-alpha knockout mice. Int J Obes Relat Metab Disord. 2002; 26:1296–1300. [PubMed: 12355324]

Lim CP, Cao X. Serine phosphorylation and negative regulation of Stat3 by JNK. J Biol Chem. 1999; 274:31055–31061. [PubMed: 10521505]

Listenberger LL, Ory DS, Schaffer JE. Palmitate-induced apoptosis can occur through a ceramide-independent pathway. J Biol Chem. 2001; 276:14890–14895. [PubMed: 11278654]

Luheshi GN, Gardner JD, Rushforth DA, Loudon AS, Rothwell NJ. Leptin actions on food intake and body temperature are mediated by IL-1. Proc Natl Acad Sci U S A. 1999; 96:7047–7052. [PubMed: 10359836]

Milanski M, Degasperi G, Coope A, Morari J, Denis R, Cintra DE, Tsukumo DM, Anhe G, Amaral ME, Takahashi HK, et al. Saturated fatty acids produce an inflammatory response predominantly through the activation of TLR4 signaling in hypothalamus: implications for the pathogenesis of obesity. J Neurosci. 2009; 29:359–370. [PubMed: 19144836]

Mistry AM, Swick AG, Romsos DR. Leptin rapidly lowers food intake and elevates metabolic rates in lean and ob/ob mice. J Nutr. 1997; 127:2065–2072. [PubMed: 9311966]

Mori H, Hanada R, Hanada T, Aki D, Mashima R, Nishinakamura H, Torisu T, Chien KR, Yasukawa H, Yoshimura A. Socs3 deficiency in the brain elevates leptin sensitivity and confers resistance to diet-induced obesity. Nat Med. 2004; 10:739–743. [PubMed: 15208705]

Obici S, Zhang BB, Karkanias G, Rossetti L. Hypothalamic insulin signaling is required for inhibition of glucose production. Nat Med. 2002; 8:1376–1382. [PubMed: 12426561]

Ozcan L, Ergin AS, Lu A, Chung J, Sarkar S, Nie D, Myers MG Jr, Ozcan U. Endoplasmic reticulum stress plays a central role in development of leptin resistance. Cell Metab. 2009; 9:35–51. [PubMed: 19117545]

Plum L, Belgardt BF, Bruning JC. Central insulin action in energy and glucose homeostasis. J Clin Invest. 2006a; 116:1761–1766. [PubMed: 16823473]

Plum L, Ma X, Hampel B, Balthasar N, Coppari R, Munzberg H, Shanabrough M, Burdakov D, Rother E, Janoschek R, et al. Enhanced PIP3 signaling in POMC neurons causes KATP channel activation and leads to diet-sensitive obesity. J Clin Invest. 2006b; 116:1886–1901. [PubMed: 16794735]

Plum L, Schubert M, Bruning JC. The role of insulin receptor signaling in the brain. Trends Endocrinol Metab. 2005; 16:59–65. [PubMed: 15734146]

Poggi M, Bastelica D, Gual P, Iglesias MA, Gremeaux T, Knauf C, Peiretti F, Verdier M, Juhan-Vague I, Tanti JF, et al. C3H/HeJ mice carrying a toll-like receptor 4 mutation are protected against the development of insulin resistance in white adipose tissue in response to a high-fat diet. Diabetologia. 2007; 50:1267–1276. [PubMed: 17426960]

Posey K, Clegg DJ, Printz RL, Byun J, Morton GJ, Vivekanandan-Giri A, Pennathur S, Baskin DG, Heinecke JW, Woods SC, et al. Hypothalamic proinflammatory lipid accumulation, inflammation, and insulin resistance in rats fed a high-fat diet. Am J Physiol Endocrinol Metab. 2008

Posey KA, Clegg DJ, Printz RL, Byun J, Morton GJ, Vivekanandan-Giri A, Pennathur S, Baskin DG, Heinecke JW, Woods SC, et al. Hypothalamic proinflammatory lipid accumulation, inflammation, and insulin resistance in rats fed a high-fat diet. Am J Physiol Endocrinol Metab. 2009; 296:E1003–E1012. [PubMed: 19116375]

Rohl M, Pasparakis M, Baudler S, Baumgartl J, Gautam D, Huth M, De Lorenzi R, Krone W, Rajewsky K, Bruning JC. Conditional disruption of IkappaB kinase 2 fails to prevent obesity-induced insulin resistance. J Clin Invest. 2004; 113:474–481. [PubMed: 14755344]

Schubert M, Gautam D, Surjo D, Ueki K, Baudler S, Schubert D, Kondo T, Alber J, Galldiks N, Kustermann E, et al. Role for neuronal insulin resistance in neurodegenerative diseases. Proc Natl Acad Sci U S A. 2004; 101:3100–3105. [PubMed: 14981233]

Schwartz MW, Porte D Jr. Diabetes, obesity, and the brain. Science. 2005; 307:375–379. [PubMed: 15662002]

Schwartz MW, Woods SC, Porte D Jr, Seeley RJ, Baskin DG. Central nervous system control of food intake. Nature. 2000; 404:661–671. [PubMed: 10766253]

Senn JJ. Toll-like receptor-2 is essential for the development of palmitate-induced insulin resistance in myotubes. J Biol Chem. 2006; 281:26865–26875. [PubMed: 16798732]

Shi H, Kokoeva MV, Inouye K, Tzameli I, Yin H, Flier JS. TLR4 links innate immunity and fatty acid-induced insulin resistance. J Clin Invest. 2006; 116:3015–3025. [PubMed: 17053832]

Shoelson SE, Lee J, Yuan M. Inflammation and the IKK beta/I kappa B/NF-kappa B axis in obesity- and diet-induced insulin resistance. Int J Obes Relat Metab Disord. 2003; 27(Suppl 3):S49–S52. [PubMed: 14704745]

Tsukumo DM, Carvalho-Filho MA, Carvalheira JB, Prada PO, Hirabara SM, Schenka AA, Araujo EP, Vassallo J, Curi R, Velloso LA, Saad MJ. Loss-of-function mutation in Toll-like receptor 4 prevents diet-induced obesity and insulin resistance. Diabetes. 2007; 56:1986–1998. [PubMed: 17519423]

Uysal KT, Wiesbrock SM, Marino MW, Hotamisligil GS. Protection from obesity-induced insulin resistance in mice lacking TNF-alpha function. Nature. 1997; 389:610–614. [PubMed: 9335502]

Weisberg SP, McCann D, Desai M, Rosenbaum M, Leibel RL, Ferrante AW Jr. Obesity is associated with macrophage accumulation in adipose tissue. J Clin Invest. 2003; 112:1796–1808. [PubMed: 14679176]

Wisse BE, Ogimoto K, Morton GJ, Williams DL, Schwartz MW. Central interleukin-1 (IL1) signaling is required for pharmacological, but not physiological, effects of leptin on energy balance. Brain Res. 2007; 1144:101–106. [PubMed: 17320056]

Won JC, Jang PG, Namkoong C, Koh EH, Kim SK, Park JY, Lee KU, Kim MS. Central Administration of an Endoplasmic Reticulum Stress Inducer Inhibits the Anorexigenic Effects of Leptin and Insulin. Obesity (Silver Spring). 2009

Woods SC, Lotter EC, McKay LD, Porte D Jr. Chronic intracerebroventricular infusion of insulin reduces food intake and body weight of baboons. Nature. 1979; 282:503–505. [PubMed: 116135]

Wunderlich FT, Luedde T, Singer S, Schmidt-Supprian M, Baumgartl J, Schirmacher P, Pasparakis M, Bruning JC. Hepatic NF-kappa B essential modulator deficiency prevents obesity-induced insulin resistance but synergizes with high-fat feeding in tumorigenesis. Proc Natl Acad Sci U S A. 2008; 105:1297–1302. [PubMed: 18216263]

Xu H, Barnes GT, Yang Q, Tan G, Yang D, Chou CJ, Sole J, Nichols A, Ross JS, Tartaglia LA, Chen H. Chronic inflammation in fat plays a crucial role in the development of obesity-related insulin resistance. J Clin Invest. 2003; 112:1821–1830. [PubMed: 14679177]

Yamamoto M, Sato S, Hemmi H, Hoshino K, Kaisho T, Sanjo H, Takeuchi O, Sugiyama M, Okabe M, Takeda K, Akira S. Role of adaptor TRIF in the MyD88-independent toll-like receptor signaling pathway. Science. 2003; 301:640–643. [PubMed: 12855817]

Yaswen L, Diehl N, Brennan MB, Hochgeschwender U. Obesity in the mouse model of pro-opiomelanocortin deficiency responds to peripheral melanocortin. Nat Med. 1999; 5:1066–1070. [PubMed: 10470087]

Zhang X, Zhang G, Zhang H, Karin M, Bai H, Cai D. Hypothalamic IKKbeta/NF-kappaB and ER stress link overnutrition to energy imbalance and obesity. Cell. 2008; 135:61–73. [PubMed: 18854155]

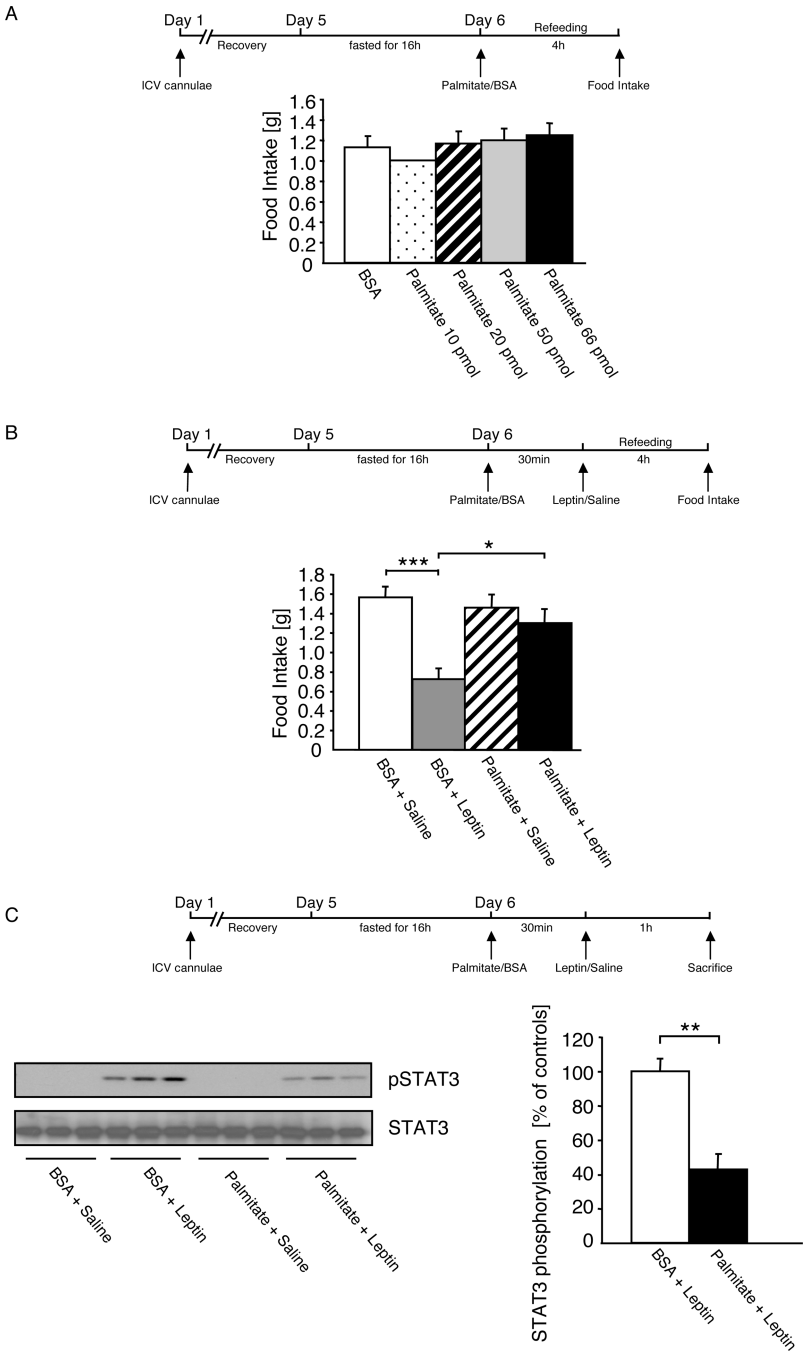

Figure 1. Acute Application of Palmitate induces Leptin Resistance in the CNS

A Food intake of 10-week-old, overnight fasted male C57/BL6 mice, which were intracerebroventricularly (ICV) injected with either vehicle (BSA) or palmitate at different concentrations (10pmol, 20pmol, 50pmol, and 66pmol), followed by refeeding for 4 hours *ad libitum* on normal diet.

B Food intake of 10-week-old, overnight fasted male C57/BL6 mice, which were ICV injected with either vehicle (BSA) or palmitate (66pmol) 30 min prior to ICV injection of leptin (500ng) or the respective vehicle (0.9% saline), followed by refeeding for 4 hours *ad libitum* on normal diet.

C Left panel: Representative western blot analysis of phosphorylated STAT3 and STAT3 (n=3) in dissected arcuate nuclei of 10-week-old, overnight fasted male C57/BL6 mice, which were ICV injected with either vehicle (BSA) or palmitate (66pmol) 30 min prior to ICV injection of leptin (500ng) or the respective vehicle (0.9% saline). Right panel: Densitometrical analysis of phosphorylated STAT3 of Palmitate + Leptin injected mice (n=7) as compared to mice injected with BSA + Leptin (n=6).
Displayed values are means ± S.E.M.; *, $p \leq 0.05$; **, $p \leq 0.01$; ***, $p \leq 0.001$.

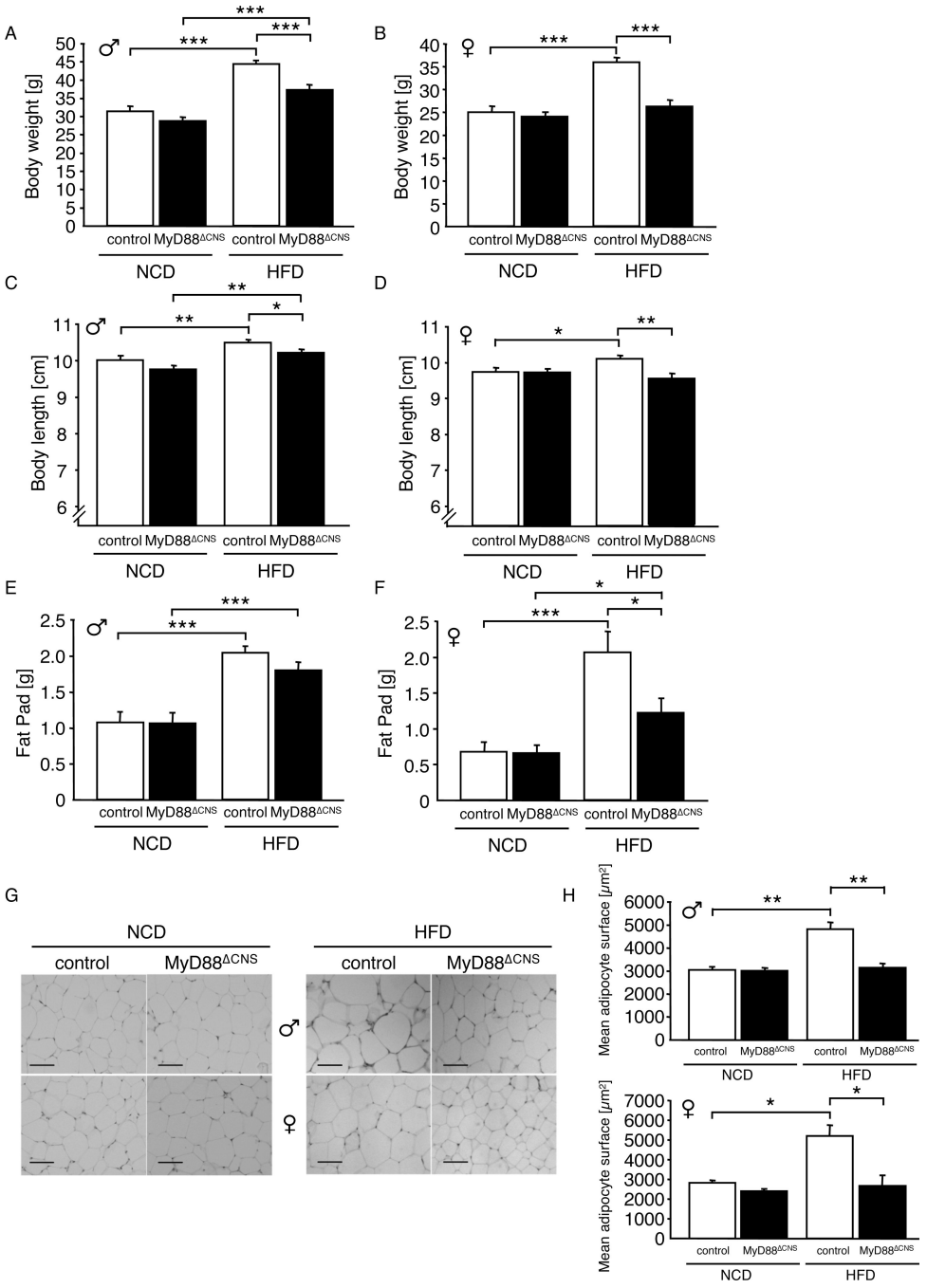

Figure 2. MyD88$^{\Delta CNS}$ mice are protected from Diet-induced Obesity

A Average body weight of male control and MyD88$^{\Delta CNS}$ mice on normal chow diet (NCD) (n=12–15) and high-fat diet (HFD) (n=11–13) at the age of 16 weeks.

B Average body weight of female control and MyD88$^{\Delta CNS}$ mice on NCD (n=12–14) and HFD (n=7–12) at the age of 16 weeks.

C Naso-anal body length of male control and MyD88$^{\Delta CNS}$ mice on NCD (n=15) and HFD (n=19–21) at the age of 16 weeks.

D Naso-anal body length of female control and MyD88$^{\Delta CNS}$ mice on NCD (n=12–14) and HFD (n=12–18) at the age of 16 weeks.

E Epididymal fat pad weights of male control and MyD88$^{\Delta CNS}$ mice on NCD (n=15) and HFD (n=19–21) at the age of 16 weeks.
F Parametrial fat pad weights of female control and MyD88$^{\Delta CNS}$ mice on NCD (n=12–14) and HFD (n=12–18) at the age of 16 weeks.
G H&E stain of epididymal/parametrial adipose tissue of male and female control and MyD88$^{\Delta CNS}$ mice on NCD and HFD at the age of 16 weeks. Scale bar: 100 μm.
H Quantification of mean adipocyte surface in epididymal/parametrial adipose tissue of male (n=3–5) and female (n=3–5) control and MyD88$^{\Delta CNS}$ mice on NCD and HFD at the age of 16 weeks.
Displayed values are means ± S.E.M.; *, $p \leq 0.05$; **, $p \leq 0.01$; ***, $p \leq 0.001$.

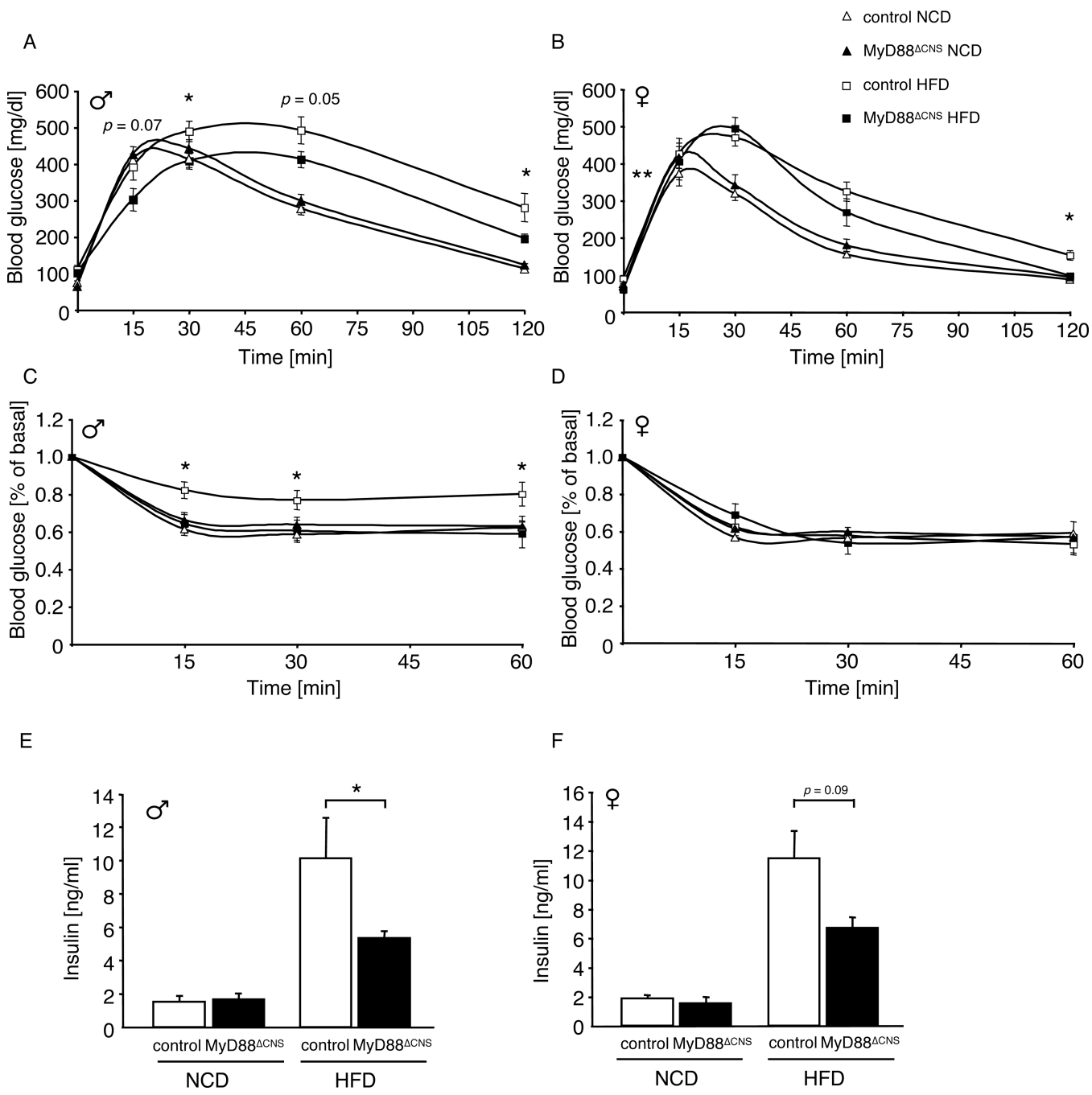

Figure 3. Improved Glucose Metabolism in MyD88$^{\Delta CNS}$ Mice on High-Fat Diet

A Intraperitoneal glucose tolerance test in male control and MyD88$^{\Delta CNS}$ mice on normal chow diet (NCD) (n=13–14) and high-fat diet (HFD) (n=11) at the age of 11 weeks.

B Intraperitoneal glucose tolerance test in female control and MyD88$^{\Delta CNS}$ mice on NCD (n=9–19) and HFD (n=7–12) at the age of 11 weeks.

C Intraperitoneal insulin tolerance test in male control and MyD88$^{\Delta CNS}$ mice on NCD (n=13–14) and HFD (n=11–13) at the age of 12 weeks.

D Intraperitoneal insulin tolerance test in female control and MyD88$^{\Delta CNS}$ mice on NCD (n=9–19) and HFD (n=7–12) at the age of 12 weeks.

E Serum insulin levels of male control and MyD88$^{\Delta CNS}$ mice on NCD (8–10) and HFD (n=11–13) at the age of 16 weeks.
F Serum insulin levels of female control and MyD88$^{\Delta CNS}$ mice on NCD (n=4–6) and HFD (n=7–12) at the age of 16 weeks.
Displayed values are means ± S.E.M.; *, $p \leq 0.05$; **, $p \leq 0.01$.

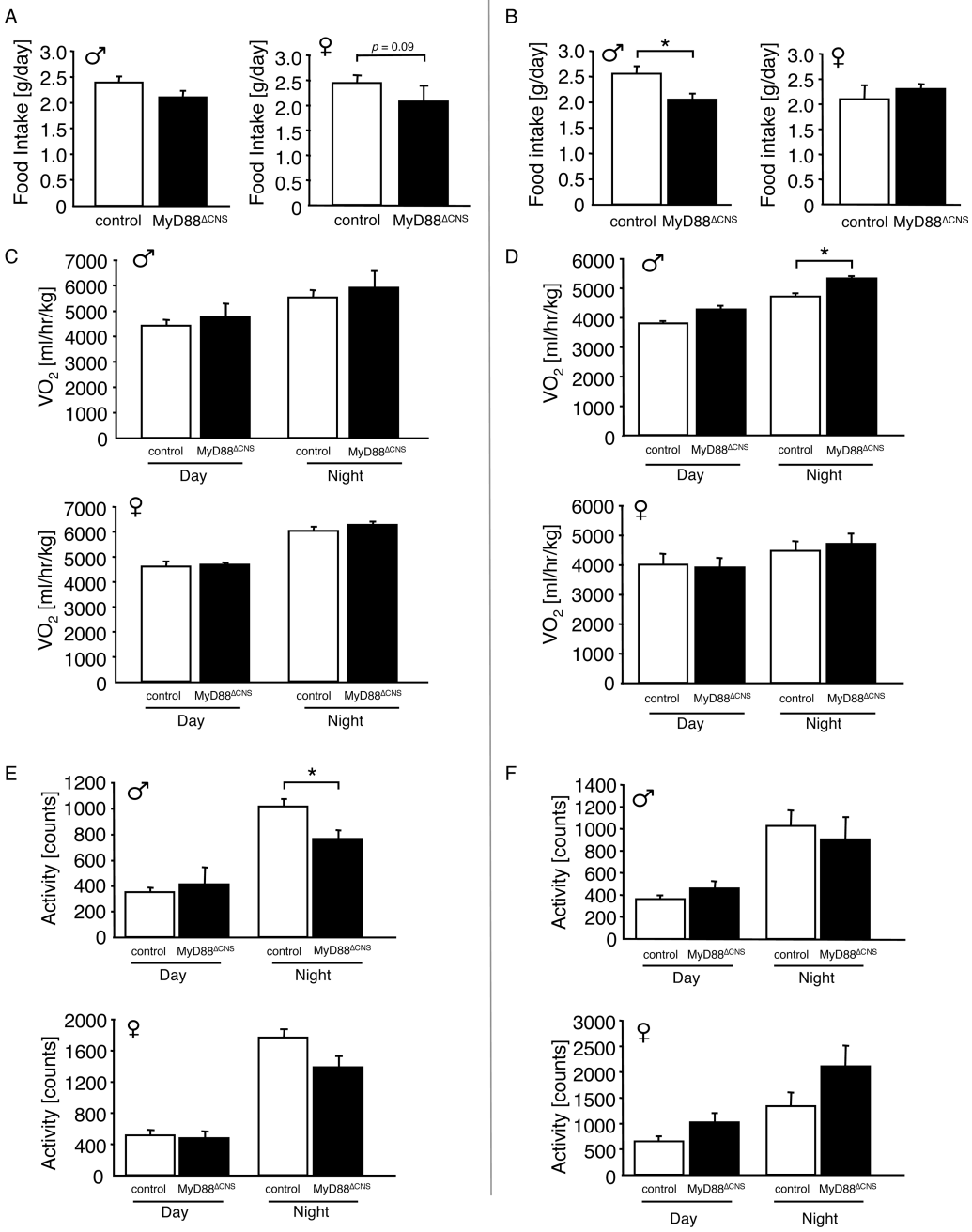

Figure 4. Decreased Food Intake in MyD88$^{\Delta CNS}$ mice on High-Fat Diet

A Daily food intake of male (n=7–14) and female (n=7–11) control and MyD88$^{\Delta CNS}$ mice on high-fat diet at the age of 4 weeks.

B Daily food intake of male (n=11–13) and female (n=5–7) control and MyD88$^{\Delta CNS}$ mice on high-fat diet at the age of 12 weeks.

C Oxygen consumption (VO_2) of male (n=7–14) and female (n=7–11) control and MyD88$^{\Delta CNS}$ mice on high-fat diet at the age of 4 weeks.

D Oxygen consumption (VO_2) of male (n=5–8) and female (n=7) control and MyD88$^{\Delta CNS}$ mice on high-fat diet at the age of 12 weeks.

E Spontaneous locomotor activity of male (n=7–14) and female (n=7–11) control and MyD88$^{\Delta CNS}$ mice on high-fat diet at the age of 4 weeks.
F Spontaneous locomotor activity of male (n=5–8) and female (n=7) control and MyD88$^{\Delta CNS}$ mice on high-fat diet at the age of 12 weeks.
Displayed values are means ± S.E.M.; *, $p \leq 0.05$.

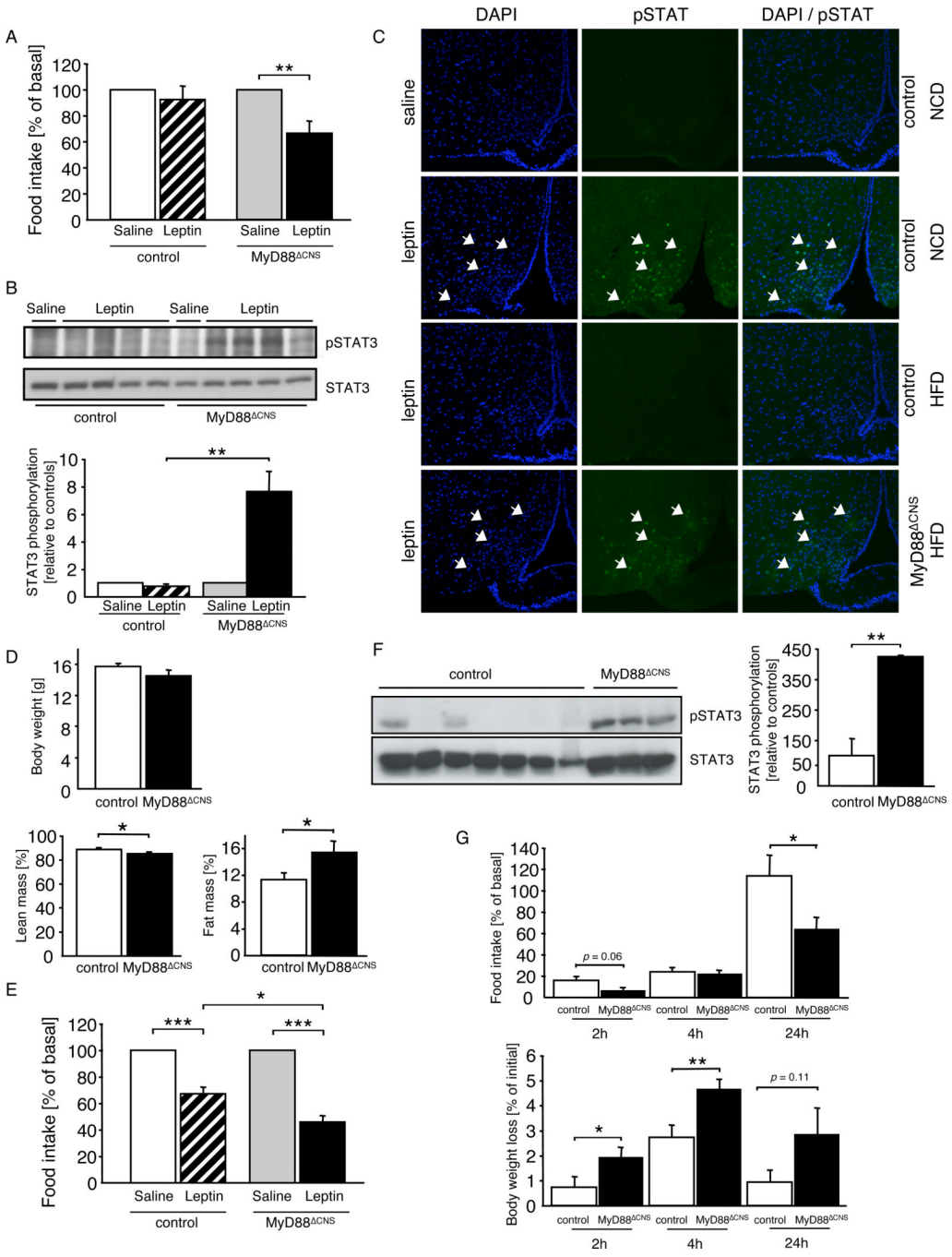

Figure 5. Enhanced Leptin Sensitivity in MyD88$^{\Delta CNS}$ Mice on High-Fat Diet

A Changes in food intake after intraperitoneal leptin treatment in control (n= 7) and MyD88$^{\Delta CNS}$ (n=7) mice on high-fat diet at the age of 14 weeks. Data represent daily food intake after a 3-day treatment with twice-daily injections of saline or 2 mg/kg leptin.

B Upper panel: Western blot analysis of phosphorylated STAT3 and STAT3 in dissected arcuate nuclei of 16-week-old control (n= 5) and MyD88$^{\Delta CNS}$ (n=5) mice, which were intravenously injected with either saline or leptin and sacrificed 30 minutes after the injection. Lower panel: Densitometrical analysis of phosphorylated STAT3 of leptin injected mice (n=4) as compared to mice injected with saline (n=1).

C pSTAT3 immunohistochemistry of ARC neurons of control and MyD88$^{\Delta CNS}$ mice on normal chow diet (NCD) or high-fat diet (HFD) was performed in overnight-fasted animals, which were intraperitoneally injected with either saline or leptin and sacrificed 30 min after stimulation. Arrows indicate neurons positive for pSTAT3 in each panel. Blue (DAPI), DNA; green, pSTAT3.
D Upper panel: Average body weight of female control and MyD88$^{\Delta CNS}$ mice on HFD (n=7–11) at the age of 5 weeks. Lower panel: Lean mass and body fat content of female control and MyD88$^{\Delta CNS}$ mice on HFD (n=7–11) at the age of 5 weeks as measured by nuclear magnetic resonance.
E Changes in food intake after intraperitoneal leptin treatment in control (n=4) and MyD88$^{\Delta CNS}$ (n=3) mice on high-fat diet at the age of 5 weeks. Data represent daily food intake after a 3-day treatment with twice-daily injections of saline or 2 mg/kg leptin.
F Upper panel: Western blot analysis of phosphorylated STAT3 and STAT3 in dissected arcuate nuclei of 10-week-old control (n=7) and MyD88$^{\Delta CNS}$ (n=3) mice, which were ICV injected with palmitate (66pmol) 30 minutes prior to ICV injection of leptin (500ng). Lower panel: Densitometrical analysis of phosphorylated STAT3 of Palmitate + Leptin injected MyD88$^{\Delta CNS}$ mice (n=3) as compared to Palmitate + Leptin injected control mice (n=7).
G Male control (n=9) and MyD88$^{\Delta CNS}$ (n=9) mice on HFD were intraperitoneally injected at the onset of the dark cyle with saline or MTII at the age of 13 weeks. Cumulative food intake and body weight were measured 2, 4, and 24 h after injection.
Displayed values are means ± S.E.M.; *, $p \leq 0.05$; **, $p \leq 0.01$; ***, $p \leq 0.001$.

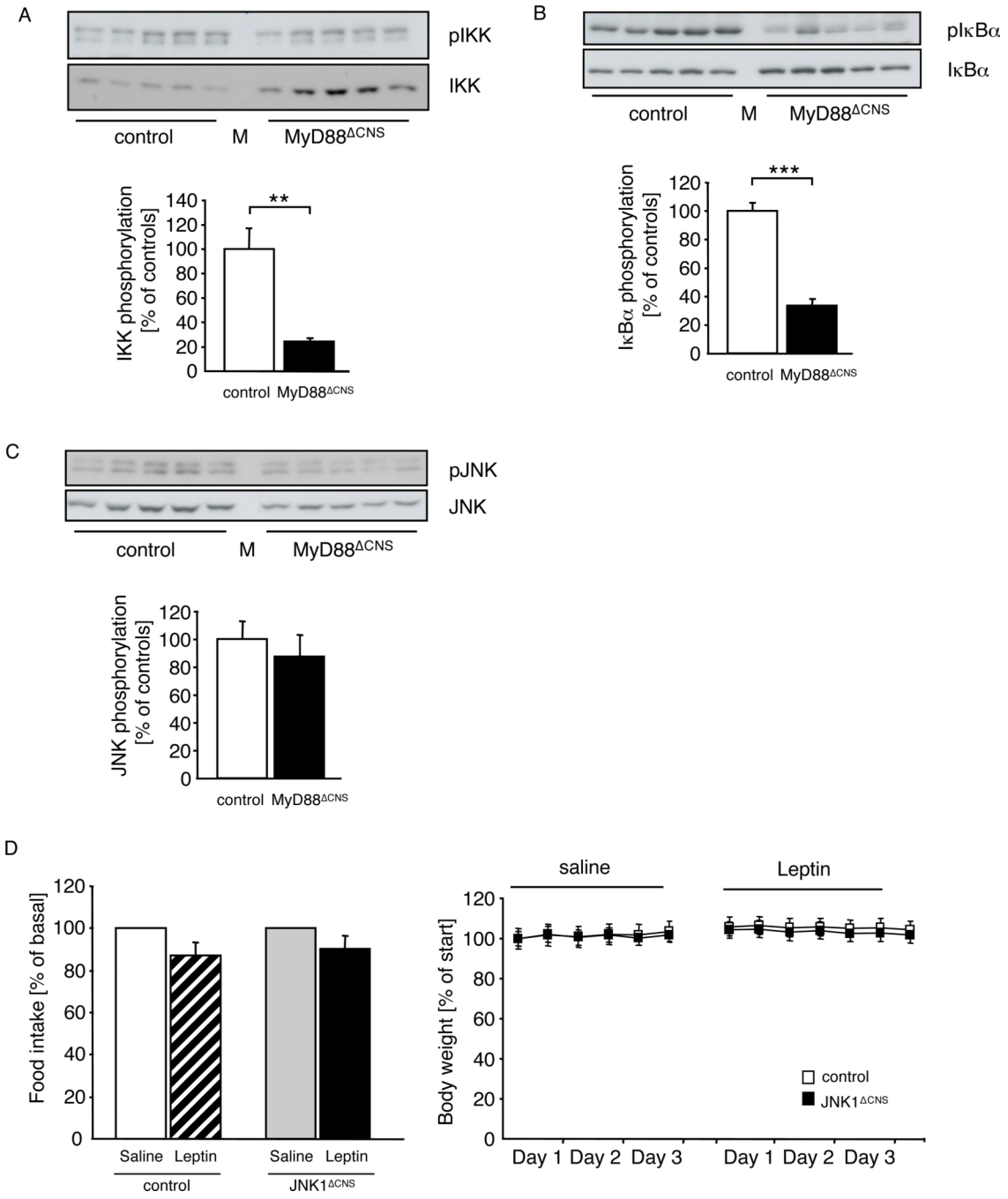

Figure 6. MyD88$^{\Delta CNS}$ mice are protected from High-Fat Diet induced IKK-activation

A Upper panel: Western blot analysis of phosphorylated IKK and IKK in dissected arcuate nuclei of 16-week-old control (n=5) and MyD88$^{\Delta CNS}$ (n=5) mice. Lower panel: Densitometrical analysis of phosphorylated IKK of MyD88$^{\Delta CNS}$ mice as compared to control mice. M: Molecular Weight Marker.

B Upper panel: Western blot analysis of phosphorylated IκBα and IκBα in dissected arcuate nuclei of 16-week-old control (n=5) and MyD88$^{\Delta CNS}$ (n=5) mice. Lower panel: Densitometrical analysis of phosphorylated IκBαof MyD88$^{\Delta CNS}$ mice as compared to control mice. M: Molecular Weight Marker.

C Upper panel: Western blot analysis of phosphorylated JNK and JNK in dissected arcuate nuclei of 16-week-old control (n= 5) and MyD88$^{\Delta CNS}$ (n=5) mice. Lower panel: Densitometrical analysis of phosphorylated JNK of MyD88$^{\Delta CNS}$ mice as compared to control mice. M: Molecular Weight Marker.
D Changes in food intake and body weight after intraperitoneal leptin treatment in control (n=8) and JNK1$^{\Delta CNS}$ (n=8) mice on high-fat diet at the age of 13 weeks. Data represent daily food intake after a 3-day treatment with twice-daily injections of saline or 2 mg/kg leptin. Body weight was measured twice a day.
Displayed values are means ± S.E.M. **, $p \leq 0.01$; ***, $p \leq 0.001$.

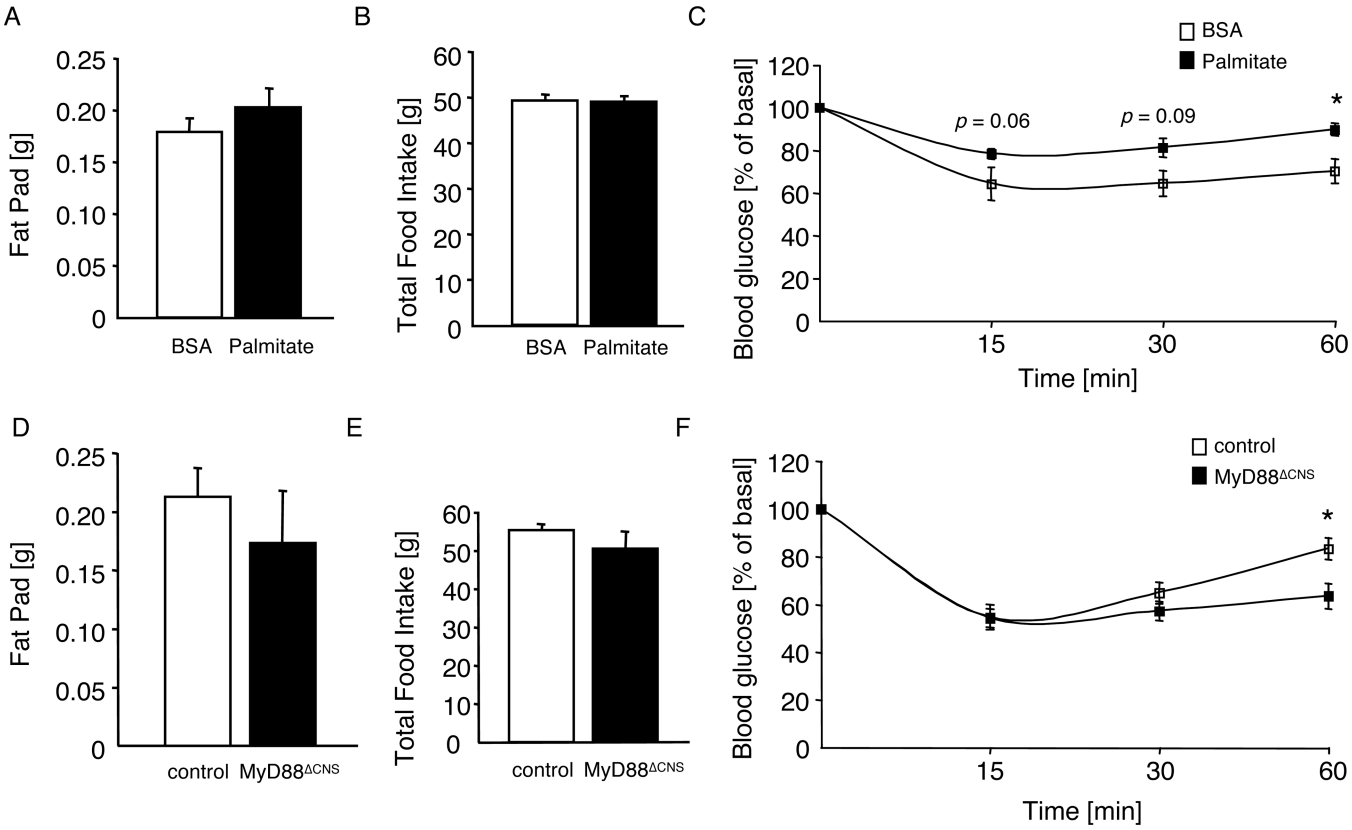

Figure 7. Palmitate-induced insulin resistance is blunted in MyD88$^{\Delta CNS}$ mice

A Epigonadal fat pad weights of wildtype mice on normal chow diet, which were chronically infused icv with either BSA (n=13) or palmitate (n=13) over a period of 2 weeks.

B Total food intake of wildtype mice on normal chow diet, which were chronically infused icv with either BSA (n=13) or palmitate (n=13) over a period of 2 weeks.

C Intraperitoneal insulin tolerance test in wildtype mice on normal chow diet, which were chronically infused icv with either BSA (n=13) or palmitate (n=13) over a period of 2 weeks.

D Epigonadal fat pad weights of control (n=15) and MyD88$^{\Delta CNS}$ (n=9) mice on normal chow diet, which were chronically infused icv with palmitate over a period of 2 weeks.

E Total food intake of control (n=15) and MyD88$^{\Delta CNS}$ (n=9) mice on normal chow diet, which were chronically infused icv with palmitate over a period of 2 weeks.

F Intraperitoneal insulin tolerance test in control (n=15) and MyD88$^{\Delta CNS}$ (n=9) mice on normal chow diet, which were chronically infused icv with palmitate over a period of 2 weeks.

Displayed values are means ± S.E.M.; *, $p \leq 0.05$.